

Self-Assembly of Microscale Objects at a Liquid/Liquid Interface through Lateral Capillary Forces

Ned Bowden, Francisco Arias, Tao Deng, and George M. Whitesides*

Department of Chemistry and Chemical Biology, Harvard University, 12 Oxford Street, Cambridge, Massachusetts 02138

Received October 16, 2000. In Final Form: December 15, 2000

Small (100–600 μm in width) hexagonal polymeric plates with faces patterned into hydrophobic and hydrophilic regions, and interacting through lateral capillary forces, were allowed to self-assemble at the perfluorodecalin/water interface. These plates were fabricated from photoresist and patterned by shadow evaporation of gold onto selected faces. The arrays that assembled from the 100 μm objects were similar in structure to those that assembled from millimeter-sized objects with analogous patterns of hydrophobic and hydrophilic faces, but with three important differences. (i) The contribution of buoyancy forces in establishing the level at which the 100 μm objects floated relative to the interface was small compared to the contribution of the vertical capillary forces. (ii) As a result, the designs of hydrophobic edges necessary to generate menisci useful in self-assembly were different for 100 μm objects than for millimeter-sized objects. (iii) The arrays that formed from the 100 μm objects had higher densities of defects than the arrays that formed from the millimeter-sized objects; these defects reflected the increase in the strength of the capillary forces (which favored assembly) relative to the shear forces (which disrupted assembly). This work adds two new elements to the study of mesoscale self-assembly: (i) It describes a new method of fabrication of plates with faces patterned into regions of different hydrophobicity that is applicable to small (perhaps $<10 \mu\text{m}$) objects, and (ii) it describes the self-assembly of 100 μm plates made by this method into ordered arrays. The work also established the contours of the menisci on the separate 100 μm and millimeter-sized plates. The scaling of the lateral and vertical capillary forces and buoyancy forces acting on millimeter-sized objects, relative to those acting on 100 μm objects, is described.

Introduction

This paper describes the self-assembly of microscopic hexagonal plates ("hexagons", having sides with dimensions of 50–300 μm and overall widths of 100–600 μm) at the perfluorodecalin (PFD)/water interface using lateral capillary forces. This work extends to these smaller objects concepts derived from studies of larger ($\sim 1 \text{ cm}$) objects. It also demonstrates fabrication techniques applicable to these smaller objects.^{1–14} We have demonstrated previously that capillary forces are effective in the self-assembly of simple polyhedral structures having sides with dimensions of several millimeters. The millimeter (mm)-sized objects used in these studies were fabricated by casting

poly(dimethylsiloxane) (PDMS) in a mold, curing the PDMS, removing the PDMS objects, oxidizing selected faces on them by exposure to a plasma, and cutting them into individual plates manually with a razor blade.³ This technique for fabrication has worked well for mm-sized objects, but we have not demonstrated that it can be scaled down to micrometer (μm)-sized objects.

We wished to have methods for fabricating objects with faces less than 1 μm in smallest dimension and for assembling them into ordered arrays. We have several reasons to wish to work with small objects. (i) Using objects with sizes of 1–10 μm , it should be possible to examine the self-assembly of large numbers ($>10\,000$) of objects and to define the order that can be achieved with such arrays. (ii) These objects have the sizes required to investigate photonic band gap materials operating in the IR range of frequencies.^{15,16}

This paper outlines several characteristics of self-assembly in intermediate-size objects that suggest approaches to self-assembly at the 1–10 μm scale. (i) We describe a method for fabricating objects with dimensions of 50–300 μm and with selected faces patterned into hydrophobic or hydrophilic regions. We believe that this method of fabrication should scale to objects with dimensions of $<10 \mu\text{m}$. (ii) We demonstrate that capillary forces can cause the self-assembly of these small plates into ordered arrays. (iii) We show that although capillary forces scale approximately with size, and although they remain useful for μm -sized objects, the relative strengths of capillary and buoyancy forces, and of capillary and shear forces, do not scale linearly with size. The behavior of systems of large and small objects in self-assembly, due to capillarity, can, as a consequence, be quite different.

(1) Wu, H.; Bowden, N.; Whitesides, G. M. *Appl. Phys. Lett.* **1999**, *75*, 3222.

(2) Bowden, N.; Terfort, A.; Carbeck, J.; Whitesides, G. M. *Science* **1997**, *276*, 233.

(3) Bowden, N.; Choi, I. S.; Grzybowski, B.; Whitesides, G. M. *J. Am. Chem. Soc.* **1999**, *121*, 5373.

(4) Bowden, N.; Oliver, S. R. J.; Whitesides, G. M. *J. Phys. Chem. B* **2000**, *104*, 2714.

(5) Breen, T. L.; Tien, J.; Oliver, S. R. J.; Hadzic, T.; Whitesides, G. M. *Science* **1999**, *284*, 948.

(6) Choi, I. S.; Bowden, N.; Whitesides, G. M. *J. Am. Chem. Soc.* **1999**, *121*, 1754.

(7) Choi, I. S.; Bowden, N. B.; Whitesides, G. M. *Angew. Chem., Int. Ed. Engl.* **1999**, *111*, 3265.

(8) Choi, I. S.; Weck, M.; Xu, B.; Jeon, N. L.; Whitesides, G. M. *Langmuir* **2000**, *16*, 2997.

(9) Huck, W. T. S.; Tien, J.; Whitesides, G. M. *J. Am. Chem. Soc.* **1998**, *120*, 8267.

(10) Oliver, S. R. J.; Bowden, N.; Whiteside, G. M. *J. Colloid Interface Sci.* **2000**, *224*, 425.

(11) Terfort, A.; Bowden, N.; Whitesides, G. M. *Nature* **1997**, *386*, 162.

(12) Terfort, A.; Whitesides, G. M. *Adv. Mater.* **1998**, *10*, 470.

(13) Tien, J.; Breen, T. L.; Whitesides, G. M. *J. Am. Chem. Soc.* **1998**, *120*, 12670.

(14) Weck, M.; Choi, I. S.; Jeon, N. L.; Whitesides, G. M. *J. Am. Chem. Soc.* **2000**, *122*, 3546.

(15) Freeman, M. H. *Optics*; Butterworth: London, 1990.

(16) Meyer-Arendt, J. R. *Introduction to Classical and Modern Optics*; Prentice-Hall, Inc.: Englewood Cliffs, NJ, 1995.

The mm-sized objects in our previous work self-assembled into complex (open, closed, linear, complete, and chiral) arrays through the interactions between the menisci on their faces.^{1,3,4,6–8,14} By patterning the faces of the objects to be either hydrophobic or hydrophilic (and, in some cases, by controlling the densities of the fluid and solid phases), we designed the objects and the contours of the menisci on the faces so that the objects assembled into well-defined, predictable arrays. The contours of the menisci are well predicted by the Laplace equation, for the simple geometries for which it can be solved (for example, for infinite slabs).^{17–22} Theory predicts that capillary forces at a liquid/liquid interface can be used to assemble objects at the nanometer (nm) and micrometer size ranges, but this prediction has not been tested in the types of systems with which we work. In related work by Nagayama and others, nm- and μm -sized spheres have been shown to self-assemble into close-packed arrays through lateral capillary forces at the liquid/air interface, but this type of self-assembly was only effective when the spheres were supported on a solid surface and the thickness of the water layer was less than the diameter of the spheres.^{19–22} This work of Nagayama et al. indicates that the capillary interactions between nm- and μm -sized objects can be sufficiently strong to cause them to self-assemble into ordered arrays, but it does not demonstrate that the structures of the arrays can be controlled by manipulating the shapes of the objects and the directionality of the forces.

The work described here represents an initial demonstration of one lithographic procedure for making small objects for self-assembly and a demonstration that simple objects prepared by this procedure do self-assemble into the expected structures. A procedure for fabrication of small objects for self-assembly must satisfy two requirements. (i) It must be able to generate large numbers ($> 10^3$) of highly uniform, μm -sized objects conveniently. (ii) It must allow the faces to be patterned into hydrophobic and hydrophilic sets.²³

Scaling of the Buoyancy and Capillary Forces with the Size of the Plates. Capillary interactions between menisci of similar shape tend to pull the objects that generate the menisci together. The motion of the objects decreases the area of the fluid/fluid interface and lowers the level of the PFD/H₂O interface; as a result, this motion decreases the free energy of the system and especially of the interface. For brevity, we call forces moving the objects “capillary forces”.^{18,24} The capillary forces can be separated into vertical and lateral components (Figure 1a). The vertical components pull the objects out of or into the interface depending on the direction of the menisci. (We call the menisci that rise above the plane of the interface “positive” menisci and the menisci that curve down below the plane of the interface “negative” menisci.) Objects with a noncentrosymmetric distribution of hydrophobic faces are tilted at the interface. The lateral components of capillarity can either attract or repel adjacent objects (Figure 1b). The rules for the interactions

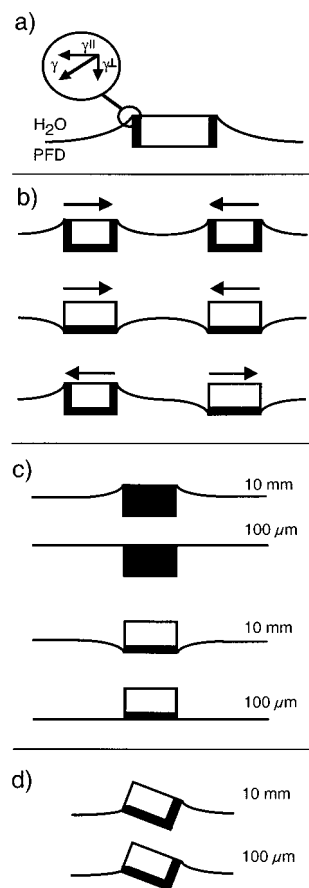


Figure 1. (a) The surface tension, γ , can be separated into horizontal, γ^{\parallel} , and vertical, γ^{\perp} , components (parallel and perpendicular to the interface, respectively). (b) Two positive menisci attract one another, two negative menisci attract one another, and a positive meniscus repels a negative meniscus. (c) Objects with mm dimensions and all sides hydrophobic (dark objects) or hydrophilic (clear objects) float partly recessed into the interface. Objects with μm dimensions and all faces hydrophobic or hydrophilic float above or below the interface and barely perturb it. (d) Objects with μm or mm dimensions and a noncentrosymmetric distribution of hydrophobic or hydrophilic faces float with a tilt relative to the interface. Some of the mm-sized hexagons tilted so far that the hydrophilic end was pulled slightly out of the interface; thus, a hydrophilic face could have a small positive meniscus due to the tilt of the hexagons. The thick lines indicate hydrophobic faces and the thin lines indicate hydrophilic faces.

of the menisci are simple: like menisci attract; unlike menisci repel. That is, two faces with positive menisci attract one another, two faces with negative menisci attract one another, and a positive meniscus is repelled by a negative meniscus.

How the objects float at the PFD/H₂O interface—their tilt and their position relative to the interface—is determined by their dimensions and pattern of hydrophobic and hydrophilic faces. The objects float at a level relative to the interface where the buoyancy and net vertical capillary forces are balanced: that is, equal in magnitude and opposite in direction. The buoyancy forces—which oppose the vertical capillary forces—scale with the volume (or the cube of the length, L^3) of the objects.^{4,18,24} In this paper and another, we present evidence that the vertical and lateral capillary forces scale approximately with the length (L) of the objects as the dimensions of the objects change from the mm to the 100 μm scale.²⁵ Thus, large

(17) Fortes, M. A. *Can. J. Chem.* **1982**, *60*, 2889.

(18) Gao, C. *Appl. Phys. Lett.* **1997**, *71*, 1801.

(19) Kralchevsky, P. A.; Paunov, V. N.; Denkov, N. D.; Ivanov, I. B.; Nagayama, K. *J. Colloid Interface Sci.* **1993**, *155*, 420.

(20) Kralchevsky, P. A.; Nagayama, K. *Langmuir* **1994**, *10*, 23.

(21) Paunov, V. N.; Kralchevsky, P. A.; Denkov, N. D.; Nagayama, K. *J. Colloid Interface Sci.* **1993**, *157*, 100.

(22) Nagayama, K.; Takeda, S.; Endo, S.; Yoshimura, H. *J. Appl. Phys.* **1995**, *34*, 3947.

(23) The method would be ideal if we could generate patterns of hydrophilic and hydrophobic areas on a single face.

(24) Chan, D. Y. C.; Henry, J. D., Jr.; White, L. R. *J. Colloid Interface Sci.* **1981**, *79*, 410.

(25) Grzybowski, B. A.; Bowden, N.; Arias, F.; Yang, H.; Whitesides, G. M. *J. Phys. Chem. B* **2001**, *105*, 404.

differences in the ratio of the buoyancy to the vertical capillary forces are possible for objects of different dimensions, and objects with similar shapes (e.g., hexagonal plates) and patterns of hydrophobic and hydrophilic faces may float at different levels relative to the interface. For similar patterns of hydrophobic and hydrophilic faces, the ratio of buoyancy to vertical capillary forces is $\sim 10^4$ smaller for 100 μm than for 10 mm objects.

For the mm-sized hexagons of PDMS floating at the interface between water and PFD, the buoyancy forces are comparable in magnitude to (although weaker than) the vertical capillary forces. Thus, the mm-sized hexagons float sufficiently high above the level of the interface to generate menisci large enough to pull them into ordered arrays. (We estimate that hexagons that are 1.2 mm thick and 5.4 mm in diameter, with all their faces hydrophobic, float with their top hexagonal face approximately 0.25 mm above the level of the interface.³) For the 100 μm hexagons, the buoyancy forces are much weaker than the vertical capillary forces. These objects with all of the faces hydrophobic or hydrophilic will not generate menisci sufficiently large that their interactions will result in self-assembly (Figure 1c). (We estimate that hexagons that are 75 μm thick and 300 μm in diameter, with all their faces hydrophobic, float with their top hexagonal face < 0.1 μm above the interface.²⁶ That is, the vertical capillary forces pull the hexagons almost entirely into the interface.)

Because buoyancy is not significant for 100 μm objects, these objects must have *both* hydrophobic and hydrophilic faces to generate menisci sufficiently large enough to allow the objects to self-assemble into ordered arrays (Figure 1c,d). Objects with both hydrophobic and hydrophilic faces will be partly recessed in the interface and will have menisci large enough to cause self-assembly. Thus, the position of a [1,3,5] hexagon relative to the plane of the interface will be determined by a competition between the vertical components of the positive and negative menisci; interactions between these menisci on separate objects will cause self-assembly roughly independent of the relative densities of the solid and liquid phases.²⁷

Objects with a centrosymmetric distribution of hydrophobic faces will float parallel to the plane of the PFD/H₂O interface. Objects with a noncentrosymmetric distribution of hydrophobic faces will float with a tilt relative to the level of the interface. These statements apply to objects with dimensions from nm to the mm (Figure 1).

Design and Fabrication of Hexagonal Plates with ~ 100 μm Lateral Dimensions. The challenge for the fabrication of these hexagonal plates was to differentiate the faces selectively into hydrophobic and hydrophilic sets. We wished to have a method that would ultimately allow us to fabricate 1–10 μm objects with hydrophobic and hydrophilic faces. Photolithography was chosen for the ease with which it can pattern complex geometries and for its ability to fabricate many different objects quickly and in parallel.²⁸ To differentiate the faces, we choose to use monolayers of alkanethiols on gold to form the

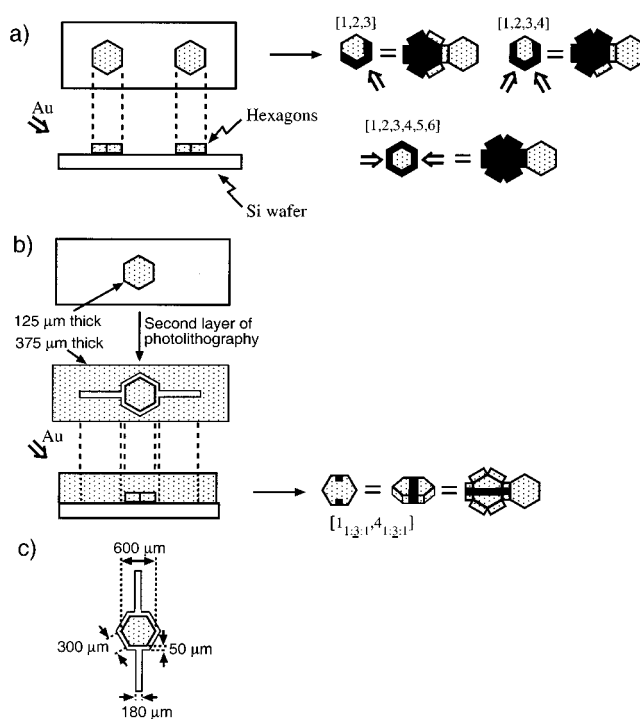


Figure 2. (a) The [1,2,3], [1,2,3,4], and [1,2,3,4,5,6] hexagons were fabricated by first patterning a layer of photoresist onto a silicon wafer. Chromium and gold were shadow evaporated onto three faces at a time; the arrows indicate the directions of the evaporations. For the [1,2,3,4] and [1,2,3,4,5,6] hexagons two evaporations were needed. We show a fold-out pattern of gold on the three hexagons; the gold is represented by the black areas. The top faces were coated with gold, and the bottom faces were not coated with gold. We do not control (or know) which face was up or down at the PFD/H₂O interface. (b) Diagram illustrating the fabrication of the [1,3,1,4,1,3,1] hexagons (the middle 60% of the [1] and [4] faces were hydrophobic; the rest was hydrophilic). First, the hexagons were patterned in photoresist. The 600 μm wide hexagons were 125 μm thick. Next, a second layer of photoresist was spun onto the wafer; this layer of photoresist was 3 times thicker than the hexagons. This layer was exposed using a correctly registered pattern and developed; after development, the original hexagons were recessed into a second, thicker layer of photoresist. Chromium and gold were shadow-evaporated through the open channel onto only one face of the hexagons at a time. A hydrophobic patch was patterned onto the face of the hexagon (indicated by the black area). The actual pattern of the Au on the top face varied with the thickness of the second layer of photoresist and the location of the hexagons in the thermal evaporator. Thus, the pattern of Au on the top face was not consistent from one hexagon to another (see Figure 7). (c) The dimensions for the photoresist in the fabrication of the [1,3,1,4,1,3,1] hexagons.

hydrophobic faces and exposed photoresist (SU-8)^{29,30} for the hydrophilic faces. We used two techniques for patterning the surfaces with gold (Figure 2). Figure 3 describes the complete process used to fabricate the hexagons.

One technique for patterning the gold on the faces (and hence for selecting the faces that would be hydrophobic) was to shadow evaporate the metal on selected faces of the hexagons.^{31,32} The hexagons were patterned by photolithography onto a silicon wafer (Figure 2a). The wafer was positioned in a thermal evaporator at an oblique angle

(26) This calculation was performed using the procedure outlined in ref 3.

(27) We number the faces by viewing the hexagons from the top. The hydrophobic faces are numbered and placed in square brackets. For instance, a [1,2,3,4] hexagon has four adjacent faces hydrophobic and the other two hydrophilic. For faces that are partly hydrophobic and partly hydrophilic, we label the pattern of hydrophobic and hydrophilic areas in the subscript. A face with the center one-third of the area hydrophobic and the rest hydrophilic is labeled as $X_{1:1:1}$; the hydrophobic area is indicated by an underline.

(28) Madou, M. *Fundamentals of Microfabrication*; CRC Press: New York, 1997.

(29) Lorenz, H.; Despont, M.; Fahrni, N.; Brugger, J.; Vettiger, P.; Renaud, P. *Sensors Actuators A* **1998**, *64*, 33.

(30) Genolet, G.; Brugger, J.; Despont, M.; Drechsler, U.; Vettiger, P.; Rooij, N. F. D.; Anselmetti, D. *Rev. Sci. Instrum.* **1999**, *70*, 2398.

(31) Olson, E.; Spalding, G. C.; Goldman, A. M.; Rooks, M. J. *Appl. Phys. Lett.* **1994**, *65*, 2740.

(32) Xia, Y.; Whitesides, G. M. *Adv. Mater.* **1996**, *8*, 765.

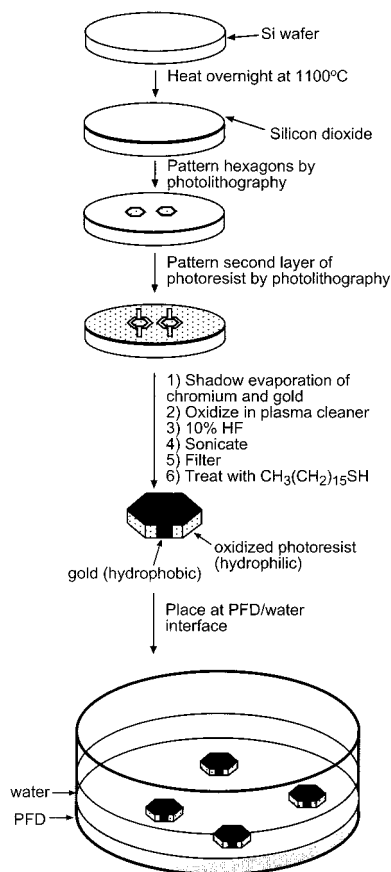


Figure 3. Fabrication of the hexagons. A thick (~ 500 nm) silicon dioxide layer was grown thermally on a silicon wafer. A layer of photoresist (SU-8) was deposited, and the wafer was patterned by photolithography (see Figure 2 for details). The wafer was positioned in a thermal evaporator at an angle of $\sim 15^\circ$ relative to the beam of gold atoms; 20 nm of chromium and 110 nm of gold were deposited. For the hexagons with channels in the second layer of photoresist, the channels were aligned with the metal source, and one evaporation was done per channel. The photoresist was oxidized by exposure to a plasma in a plasma cleaner (5 min at medium power) to make the polymer surfaces not covered with gold hydrophilic. The silicon dioxide layer was dissolved in 10% HF to release the photoresist from the surface. The wafer was placed in a cup with water and briefly sonicated to separate the hexagons from the wafer. The hexagons were isolated by filtration, dried, soaked in a 2 mM ethanolic solution of $\text{HS}(\text{CH}_2)_{15}\text{CH}_3$ for 10 min, and dried. The gold-coated areas were hydrophobic; the exposed photoresist was hydrophilic. The hexagons were suspended in a drop of water with a pipet and transferred to the PFD/ H_2O interface. The dish was 6.5 cm in diameter and contained 50 mL of PFD and 40 mL of water. The dish was agitated on an orbital shaker in the plane of the PFD/ H_2O interface.

to the metal source. The wafer was not spun during the evaporation; as a result, only three faces were exposed to the Cr and Au at any one time. Chromium and gold were shadow evaporated onto only three side faces and the top face of the hexagons. This technique was used to fabricate the [1,2,3], [1,2,3,4], and [1,2,3,4,5,6] hexagons.

The second technique for patterning the gold involved fabricating a second, thicker layer of photoresist around the hexagons. First, we fabricated a set of hexagons on a silicon wafer using photolithography as before. (The photoresist was 125 μm thick for the 600 μm wide [1_{1:3:1}, 4_{1:3:1}] hexagons.) Next, we spun a second, thicker layer of photoresist (375 μm thick for the 600 μm wide [1_{1:3:1}, 4_{1:3:1}] hexagons) onto the wafer and aligned a mask over the embedded pattern of hexagons. The photoresist

was exposed through the mask and developed; the second, thicker layer of photoresist formed a series of slots around the hexagons as shown in Figure 2b. The face that was to be coated with Au had a slot in the photoresist perpendicular to the face. The slot provided a path for the Cr and Au to deposit onto the face. The silicon wafer with the two layers of patterned photoresist was placed in the thermal evaporator with one slot aligned with the metal source, and chromium and gold were shadow evaporated onto the wafer. The chromium and gold only deposited on the face with the slot aligned with the beams. Each face with a slot required a separate evaporation. The faces that were to be rendered hydrophilic were shielded from the Au by the thick layer of photoresist around the hexagons. This technique was used to fabricate the [1_{1:3:1}, 4_{1:3:1}] hexagons.

The exposed photoresist was rendered hydrophilic by oxidation in a plasma cleaner.^{28,33,34} After oxidation, the faces coated with gold were made hydrophobic by allowing a self-assembled monolayer of hexadecanethiol to form on them (Figure 3).^{35–37} The hexagons were placed at the interface by suspending them in water and pipetting the solution onto the interface. We did not control whether the hexagonal face coated with gold or the hexagonal face of oxidized photoresist was in contact with the water. We could not determine which hexagonal face was up or down at the interface because of the opacity of the photoresist and the small amount of Cr used as an adhesion layer between the Au and photoresist. For a glass slide with a Cr adhesion layer between the Au and the glass, we can determine which face had Au on it by viewing the color of the Au. (The Au appears darker when viewed through Cr than when it is viewed without a layer of Cr.) In our system, the Cr layer was too thin to provide a reliable way of distinguishing which hexagonal face was up or down at the interface. For these experiments we do not expect any difference in the arrays that formed based on which hexagonal face was in contact with the water layer, because which hexagonal face was in contact with the H_2O did not affect the menisci nor did it affect the tilt of the hexagons. At no point in the fabrication were the hexagons handled individually or with tweezers.

We believe that the procedures outlined can be used to fabricate objects much smaller than those shown, although generation of the masks and registration present technical problems. The size of the objects was limited by our methods of generating masks for the photolithography and the limits of accuracy in registration of the second mask to pattern the background layer of photoresist. Briefly, the design of the mask was printed at high resolution; at this point the hexagons were 10 \times or 25 \times their final size (that is, 1.0–2.5 mm in length).^{38,39} The print was photographed onto microfiche; this process reduced the size of the features by 10 \times or 25 \times . The microfiche was used as a contact mask for the photolithography. For hexagons requiring a second, thicker layer of photoresist, the pattern for the second layer of photoresist was registered with the first pattern by hand and eye; this method limited us to using objects several

(33) Chou, N. J.; Tang, C. H.; Paraszcak, J.; Babich, E. *Appl. Phys. Lett.* **1985**, *46*, 31.

(34) Bowden, N.; Huck, W. T. S.; Paul, K. E.; Whitesides, G. M. *Appl. Phys. Lett.* **1999**, *75*, 2557.

(35) Delamar, E.; Michel, B.; Biebuyck, H. A.; Gerber, C. *Adv. Mater.* **1996**, *8*, 719.

(36) Delamar, E.; Michel, B. *Thin Solid Films* **1996**, *273*, 1123.

(37) Poirer, G. E. *Chem. Rev.* **1997**, *97*, 1117.

(38) Xia, Y.; Whitesides, G. M. *Angew. Chem., Int. Ed. Engl.* **1998**, *37*, 550.

(39) Qin, D.; Xia, Y.; Black, A. J.; Whitesides, G. M. *J. Vac. Sci. Technol., B* **1998**, *16*, 98.

hundred μm in size. With commercial chrome masks and improved methods of registration, we believe that this method of fabrication will scale down by approximately 2 orders of magnitude in size (to hexagons a few μm in diameter and $\sim 0.5 \mu\text{m}$ thick).

Differences in the Contact Angles and Densities of the mm- and 100 μm -Scale Hexagons. There are four characteristics of the materials used to fabricate the hexagons (PDMS for the mm-sized hexagons; photoresist and C_{16} SAMs for the 100 μm hexagons) that could affect their assembly. (i) The dimensions of the side faces determine the decay length of the menisci for the PFD/ H_2O interface. The decay lengths of the menisci are very different for the mm- and μm -sized hexagons. (ii) The contact angles of H_2O on the PDMS and the hydrophobic SAM determine how well the PFD wets these faces and how high the menisci rise. The contact angle of water on PDMS was 108° and on the hydrophobic SAM was 110° . These numbers are indistinguishable; hence, the wetting of PFD on the hydrophobic surfaces will be similar for the mm- and 100 μm -scale hexagons. (iii) The contact angles of H_2O on the oxidized PDMS and oxidized photoresist were both $< 30^\circ$. These surfaces are both hydrophilic and will be wet similarly by H_2O . (iv) The density of the PDMS was 1.05 g cm^{-3} , and the density of the photoresist was 1.1 g cm^{-3} . This small difference in density is unimportant in comparing the arrays that assemble from the mm-sized hexagons with the arrays that assemble from the 100 μm hexagons. Because the materials used in the assembly of the mm and 100 μm hexagons had similar wettabilities and densities, we believe that the differences in the arrays are determined by the differences in the sizes of the hexagons.

Experimental Section

All evaporations were done in a Edwards Auto 306 thermal evaporator. In a typical evaporation, 20 nm of Cr and 110 nm of Au were deposited. The hexagons were oxidized in a Harrick PDC-23G plasma cleaner at medium power for 5 min: this oxidation rendered the exposed photoresist hydrophilic (the advancing contact angle of water was $\theta_a < 30^\circ$). The oxidized photoresist remained hydrophilic after exposure to air or under H_2O for intervals of more than a week. The photoresist used was SU8-50 (purchased from Microchem Co., Newton, MA). Hexadecanethiol was purchased from Aldrich and passed through a column of silica gel before use.

Measurement of the Contours of the Menisci.²⁵ The hexagons were placed in a cylindrical container 6.5 cm in diameter with 30 mL of PFD and 30 mL of H_2O . The dish was placed in a cold room at 3°C . Gelatin (type A from porcine skin, 300 bloom, purchased from Aldrich) was added to water at a concentration of 9 g of gelatin per 100 mL of H_2O . The water/gelatin was heated to 90°C to dissolve the gelatin, and 30 mL of gelatin solution was slowly added over a period of 1 min to the container with the hexagons. The system was allowed to gel for at least 3 h at 3°C . The gelatin was removed and blown dry with N_2 for 10 s, and Norland Optical Adhesive (NOA) was poured on the gelatin and cured under UV light. The gelatin was removed from the NOA by dissolving it in warm water. The NOA was a replica of the PFD/ H_2O interface and thus of the menisci of PFD. The menisci measured using this method slightly differed from the menisci at the gelatin-free PFD/ H_2O interface. (The gelatin lowered the interfacial free energy of the PFD/ H_2O interface.) These differences are small: we note that they exist, and we will discuss them elsewhere.²⁵

Results

[1,2,3] Hexagons. We prepared three sets of [1,2,3] hexagons with different sizes (100 μm wide and 30 μm thick; 100 μm wide and 50 μm thick; and 300 μm wide and 75 μm thick) and compared the arrays that they formed

to those that assembled from [1,2,3] hexagons that were 5.4 mm wide and 1.2 mm thick.³ Previous studies of mm-sized hexagons (Figure 4a,b) had shown that (i) they were tilted at the interface by 15° , (ii) they assembled into approximately a 1:1 mixture of cyclic and linear arrays through interactions between opposing faces and opposing vertexes, and (iii) the [2] face was pulled into the interface so far that it did not generate menisci large enough to assemble into contact with other faces.

The 300 and 100 μm hexagons assembled primarily into lines interacting at vertexes, with $< 10\%$ of hexagons also present in the cyclic arrays. The 300 μm hexagons were agitated at $\omega = 1.5\text{--}1.8 \text{ s}^{-1}$; these hexagons assembled into lines with most of the [2] faces on the same side of the line. The 100 μm hexagons were agitated at a range of frequencies (and, thus, intensities of agitation) from $\omega = 1.5 \text{ s}^{-1}$ (at which frequency they assembled in the center of the dish) to $\omega = 1.8 \text{ s}^{-1}$ (at which frequency they assembled over the whole dish). The lines of the 100 μm wide and 30 μm thick hexagons had more defects (the "trans" configuration labeled as A in Figure 4) than did the 100 μm wide and 50 μm thick hexagons. Previous studies of mm-sized hexagons had established that the trans arrangement of hexagons was less favored than the cis because it matched the contours of the menisci less well (Figure 5). We note that although the 100 μm , 300 μm , and mm-sized hexagons assembled into different proportions of linear and cyclic arrays, the basic structures of the arrays were the same for these three sizes.

The hexagons were tilted at the PFD/ H_2O interface and had menisci that were noncentrosymmetric. The 100 and 300 μm hexagons assembled predominately into lines, while the mm-sized hexagons assembled into a $\sim 1:1$ mixture of lines and cyclic arrays. There are at least three possible reasons for this difference. (i) *The 100 and 300 μm hexagons responded differently to the agitation than the mm-sized hexagon.* We cannot rule out this possibility, but it is unlikely. The hexagons were agitated on the same orbital shaker; the shear and other forces breaking the arrays apart should be similar. Also, we believe that the form of arrays that are generated are determined more by the pattern of the hydrophobic faces and less by the agitation. (ii) *The rates of formation of cyclic arrays of 100 and 300 μm hexagons are much slower than those of linear arrays.* The mm-sized hexagons rapidly equilibrated (< 30 min) into a mixture of linear and cyclic arrays, but we do not know whether the arrays of the 100 and 300 μm hexagons were equilibrated. It is possible that the linear arrays assembled first and the 100 and 300 μm hexagons did not reassemble into the cyclic arrays. (iii) *The contours of the menisci on the 100 and 300 μm hexagons were different from the mm-sized hexagons.* We have not measured the contours of the menisci with enough accuracy to determine whether this hypothesis might be correct, but we believe that there are differences between the menisci on the hexagons. Because the ratio of the buoyancy to the vertical capillary forces is much smaller for the 100 and 300 μm than the mm-sized hexagons, the tilt of these hexagons at the interface will differ, and the contours of the menisci will be different for the 100 and 300 μm and mm-sized hexagons and may lead to a different distribution of linear and cyclic arrays.

[1,2,3,4] Hexagons. We fabricated [1,2,3,4] hexagons that were 100 μm wide and 30 and 50 μm thick. We compared these arrays to those that assembled from [1,2,3,4] hexagons that were 5.4 mm wide and 1.2 mm thick (Figure 6a). The mm-sized hexagons were tilted at the interface by 14° ; they assembled into lines based on the interactions between the [1] and [4] faces. The [2] and

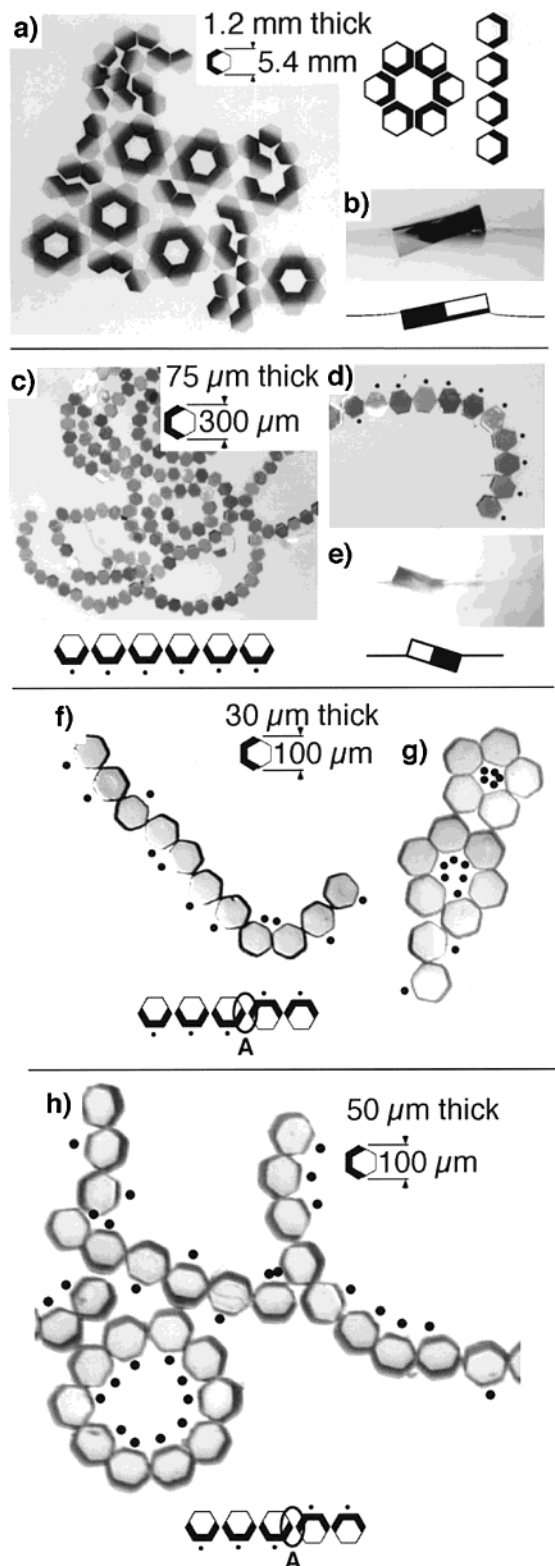


Figure 4. (a) The mm-sized [1,2,3] hexagons assembled into lines and cyclic arrays. The dark faces are hydrophobic, and the light faces are hydrophilic. (b) The hexagon from the side shows the tilt. (c–e) The arrays that assembled from the 300 μm wide [1,2,3] hexagons. (e) The hexagon from the side shows the tilt. The dots in (d), (f), (g), and (h) were added manually to the figure. They are adjacent to the [2] faces of the hexagons and are meant as an aid to the eye. (f, g) The 100 μm wide and 30 μm thick hexagons assembled mostly into lines with a few cyclic arrays. The lines assembled with the [2] faces on the hexagons on either side of the lines. The 100 μm wide and 50 μm thick hexagons assembled into mostly into lines with a few cyclic arrays

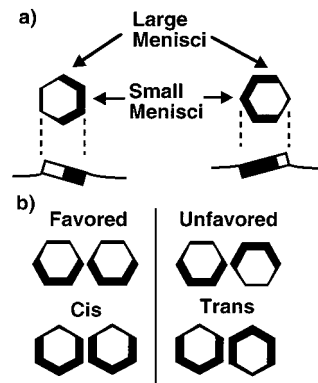


Figure 5. (a) The [1,2,3] and [1,2,3,4] hexagons are tilted at the interface and the heights of the positive menisci differ along the faces. (b) The [1,2,3] and [1,2,3,4] hexagons can assemble into the cis or trans configurations. The cis configuration matches the heights of the menisci on opposing faces and is favored. The trans configuration does not allow the contours of the menisci to match on opposing faces and is disfavored.

[3] faces were buried into the interface and had smaller menisci than those on the [1] and [4] faces. From experiments with the mm-sized hexagons, we knew that cis orientation was favored over the trans orientation (Figure 5).³

The 100 μm hexagons also assembled into lines based on the interactions between the [1] and [4] faces (Figure 6). The 30 μm thick hexagons had more irregularities and errors in the assemblies (structures labeled B in Figure 6) than the 50 μm thick hexagons. The lines and defects were stable to high rates of agitation ($\omega = 1.8 \text{ s}^{-1}$); we could not anneal the defects out of the arrays.

To investigate the strength of the interaction between the 100 μm wide [1,2,3,4] hexagons, we studied them under a low power microscope. Two hexagons were separated using tweezers and allowed to assemble together. The hexagons rapidly came into contact ($\sim 1 \text{ s}$) from separations up to several diameters of the hexagons. Hexagons that were in the disfavored trans orientation did not rotate with respect to one another before coming into contact. The hexagons appeared to be held together by strong interactions even for the disfavored orientations. (The hexagons did not readily dissociate upon agitation on an orbital shaker, although mm-sized hexagons in the trans configuration readily dissociated under agitation.) We surmise from the optical micrographs that the hexagons only slowly dissociate on the time scale of the experiment even after assembling into disfavored orientations.

The arrays that assembled from the 100 μm and mm-sized hexagons had a number of similarities. (i) Both sets of the hexagons were tilted at the interface. (ii) Both sets of the hexagons assembled into lines based on interactions between the [1] and [4] faces with the [2] and [3] faces on the same side of the lines. (iii) These lines further assembled into loose aggregates. A difference between the arrays of the 100 μm and mm-sized hexagons was that the lines of the 100 μm hexagons incorporated more hexagons than did the lines of mm-sized hexagons.

[1_{1:3:1},4_{1:3:1}] Hexagons. We assembled [1_{1:3:1},4_{1:3:1}] hexagons that were 600 μm wide and 125 μm thick (Figure 7). These hexagons assembled into lines similar to those formed by [1,4] hexagons that were 5.4 mm wide (Figure 7a). The formation of lines from the 600 μm hexagons demonstrates that objects that have faces that have been patterned using the techniques outlined in Figure 2 self-assemble.

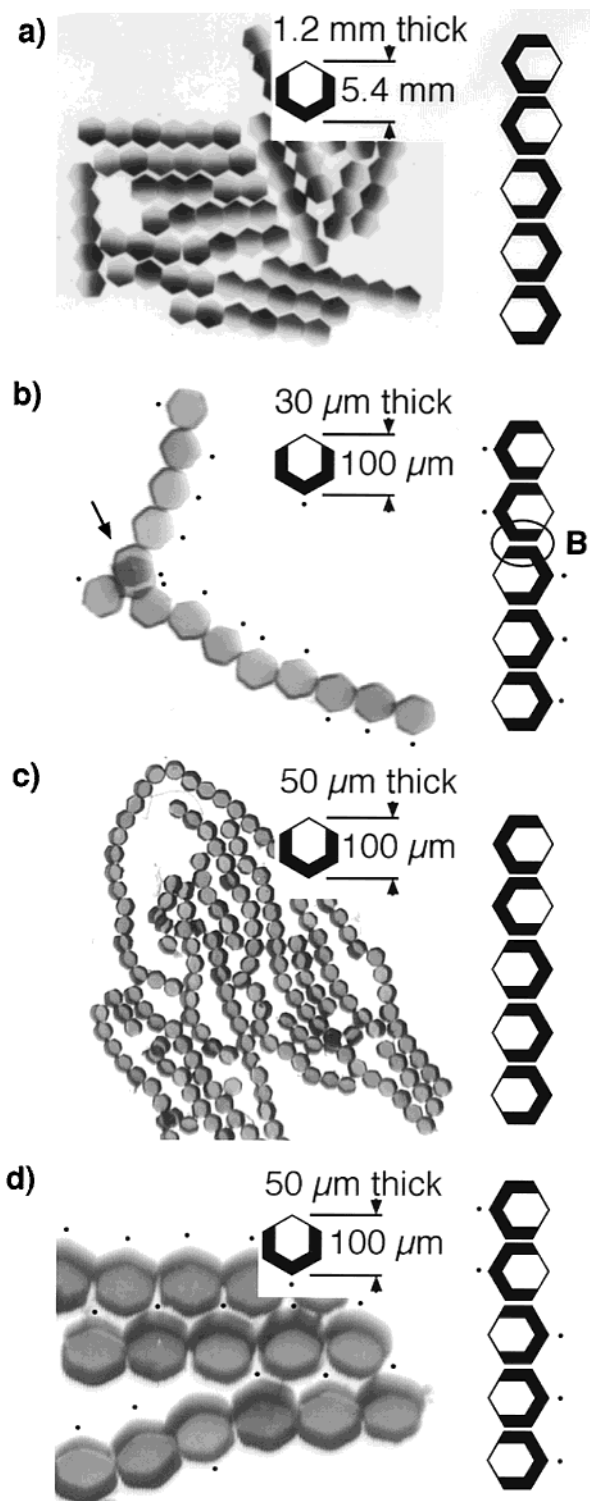


Figure 6. (a) The mm-sized hexagons assembled into lines that aggregated together when the agitation was stopped. (b) The $100\ \mu\text{m}$ wide and $30\ \mu\text{m}$ thick hexagons assembled into lines based on interactions between the [1] and [4] faces. The arrow points to two hexagons that were stacked on one another. (c) Typical arrays of hexagons and (d) a close-up of an array. The dots were manually added to (b) and (d) as an aid to the eye. The dots are adjacent to the vertices between the [2] and [3] faces.

The top faces of the hexagons had different patterns of Au due to different shadowing effects from the evaporation of the metals on the hexagons. The thickness of the second layer of photoresist and the placement of the hexagons with respect to the metal sources varied in the evaporation

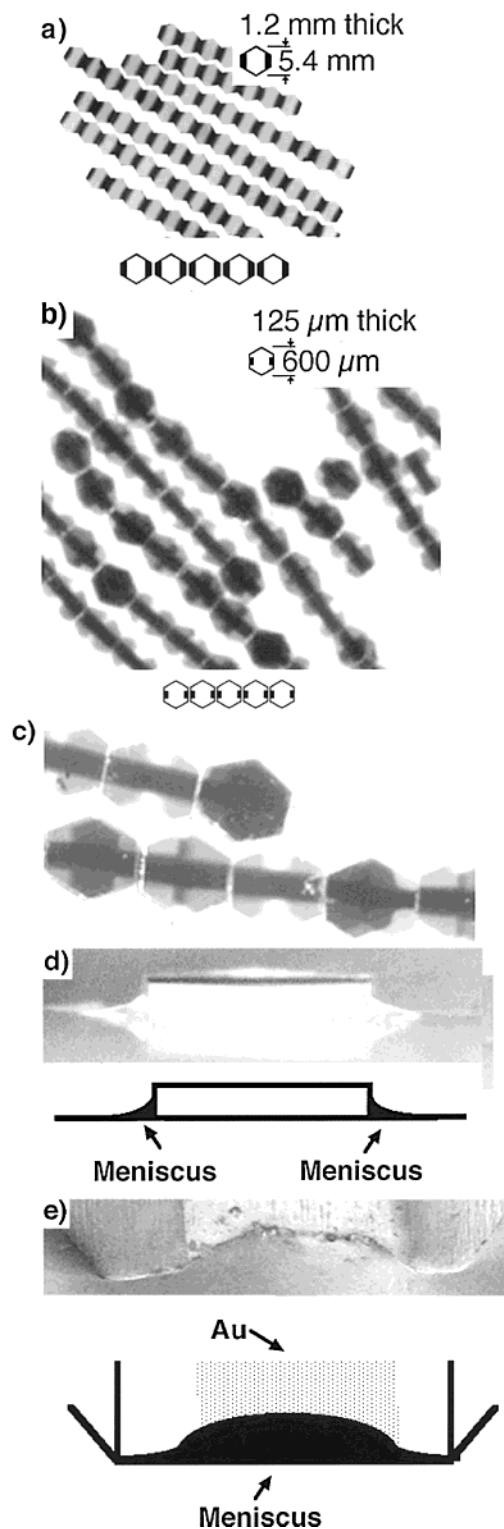


Figure 7. (a) The mm-sized hexagons assembled into lines. The dark faces are hydrophobic and the light faces are hydrophilic. (b, c) The $600\ \mu\text{m}$ hexagons also assembled into lines. The dark line on the top face of the hexagons that is parallel to the direction of the array indicates where the Au is on the [1_{1:3:1}] and [4_{1:3:1}] faces of the objects. (d) An optical image of the replica—fabricated according to the procedure in the text—in NOA of the menisci shows the menisci on the [1_{1:3:1}] and [4_{1:3:1}] faces. A figure of the hexagon and PFD/H₂O interface is beneath the optical micrograph. (e) A scanning electron microscope image of the replica in NOA shows the menisci along the face of a hexagon. The image is from the top at an angle. A figure of the hexagon and PFD/H₂O interface is beneath the SEM. We note that the PFD does not wet the entire face in either (d) or (e).

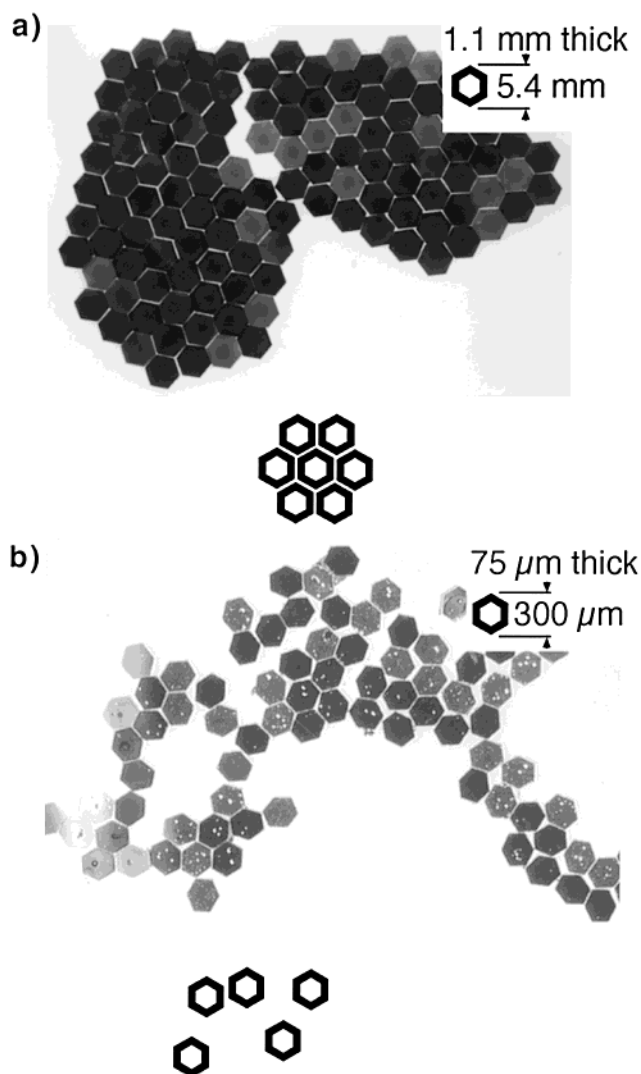


Figure 8. (a) The mm-sized, [1,2,3,4,5,6] hexagons assembled into close-packed arrays. (b) The corresponding μm -sized hexagons assembled into loose aggregates.

chamber; thus, the pattern of Au on the top faces was not consistent from one hexagon to another. The Au on the top faces varied from mostly clear to black due to these differences and to the fact that the photoresist was (mostly) transparent. We note that the pattern of Au on the top face did not affect the placement of the Au on the side faces. In most of the hexagons, there was a strip of Au (which appears black in Figure 7) on the top face that indicated where the Au was on the two side faces of the hexagons. We note that these strips of Au opposed one another on hexagons that came into contact.

Imaging the Shape of the Menisci. We wished to image the menisci on the $600\ \mu\text{m}$ wide [1_{1:3:1}, 4_{1:3:1}] hexagons to learn how the contours compare to the menisci on the mm-sized hexagons. Specifically, we wished to know how the contact angle of PFD on the hydrophobic faces and the decay lengths of the menisci scaled as we changed the dimensions of the objects. From the contact angles on the $600\ \mu\text{m}$ and the mm-sized hexagons we can learn how the lateral and vertical capillary forces scaled with the dimensions of the objects. This scaling is possible because the contact angle allows the separation of the vertical and lateral components of the capillary force (Figure 1a); by knowing the contact angle, we therefore have an estimate of the capillary force per unit length of the objects. A

comparison of the decay lengths of the menisci from the $600\ \mu\text{m}$ and mm-sized hexagons would describe how far from the face of the objects the menisci would be felt by other menisci. To image the menisci, we fabricated replicas of the PFD/H₂O interface as described in the Experimental Section.

The decay lengths measured from the gelatin replicas are approximately $90\ \mu\text{m}$ for hexagons with edges that are $600\ \mu\text{m}$ wide and $900\ \mu\text{m}$ for a similarly patterned hexagon with faces that are $5.4\ \text{mm}$ wide. Thus, the decay length dropped by an order of magnitude when the width of the face was dropped by an order of magnitude. In addition, the contact angles of the PFD/H₂O interface on the hydrophobic faces of the μm - and mm-sized hexagons were similar (*both were approximately 59°*). We surmise that the lateral and vertical capillary forces per unit length on the $600\ \mu\text{m}$ and mm-sized hexagons are the same. Thus, we have a method for estimating how the energy of interaction between two objects scales with their dimensions.

[1,2,3,4,5,6] Hexagons. We assembled [1,2,3,4,5,6] hexagons that were $300\ \mu\text{m}$ wide and $75\ \mu\text{m}$ thick (Figure 8). These hexagons did not assemble into ordered arrays; they aggregated only loosely with one another. This result is in contrast to the [1,2,3,4,5,6] hexagons that were $5.4\ \text{mm}$ wide and $1.1\ \text{mm}$ thick; these hexagons assembled into one or more large, close-packed arrays (Figure 8). As we have discussed previously, we believe that the differences in these arrays originate in the balance between the vertical capillary and the buoyancy forces and the differences in this balance between large and small hexagons. For the $300\ \mu\text{m}$ hexagons, the buoyancy forces are much weaker than the vertical capillary forces, and the hexagons do not perturb the interface enough to generate menisci sufficiently large to cause self-assembly.

Conclusions

Hexagons with $\sim 100\ \mu\text{m}$ Dimensions, and with Faces Patterned into Hydrophobic and Hydrophilic Sets, Self-Assemble into Ordered Arrays. We have demonstrated two techniques for fabricating objects with $100\ \mu\text{m}$ dimensions that have faces patterned to be hydrophobic or hydrophilic. These techniques have been applied to objects with dimensions of $50\text{--}300\ \mu\text{m}$, and we have fabricated objects with four different patterns of hydrophobic and hydrophilic faces. We believe that these methods can be used to fabricate objects with patterned faces and dimensions of $1\text{--}10\ \mu\text{m}$. Currently, our method for registering the mask for the second layer of photoresist limits the size of the objects that we can readily fabricate. Using standard methodologies for semiconductor device fabrication, however, we would anticipate being able to fabricate patterned objects with $\sim 1\ \mu\text{m}$ wide faces.²⁸

The structures of arrays that self-assembled from these objects were largely predicted by analogy with the arrays that assembled from the mm-sized hexagons, although the arrays formed from [1,2,3,4,5,6] hexagons were quite different for the two sizes. Some of the differences in the arrays can be partly attributed to the differences in the balance of the vertical capillary forces and buoyancy forces acting on the objects. For the mm-sized objects, the vertical capillary forces were comparable in magnitude to the buoyancy forces; for the $100\ \mu\text{m}$ objects, the vertical capillary forces were much greater than the buoyancy forces. Thus, the tilt or level of the hexagons relative to the interface, and thus the form of the menisci, differed for the $100\ \mu\text{m}$ and mm-sized hexagons.

The $\sim 100\ \mu\text{m}$ Hexagonal Plates Assembled into Arrays That Were More Disordered Than the Arrays

That Assembled from the mm-Sized Plates. The arrays that assembled from the $\sim 100\ \mu\text{m}$ hexagons were kinetic products; defects were not annealed on continued agitation. Capillary interactions favoring assembly were much larger than shear interactions disrupting assembly in these smaller systems. In contrast, the errors in the assembly of the arrays of the mm-sized hexagons could be largely removed by annealing. The assemblies of the mm-sized hexagons could be made to be reversible, whereas the assemblies of the μm -sized hexagons were mostly irreversible. At rates of agitation where the μm -sized hexagons freely dissociated from one another, the interface was turbid (as a result of formation of bubbles at the interface); this roughness at the interface prevented the self-assembly of highly ordered aggregates.

Why are the defects in the arrays of the mm-sized hexagons more easily removed by annealing than the errors in the array of the $100\ \mu\text{m}$ hexagons? We believe that the capillary forces favoring assembly scale differently than the shear forces opposing assembly. The lateral capillary forces (those that hold the objects in contact) scale approximately with the length of the μm - and mm-sized hexagons. The shear forces (those that oppose the lateral capillary forces) scale with the length to a higher power than one. We do not know exactly how the shear forces scale with the length of the objects, but indirect evidence supports our claim that the shear forces were too weak to equilibrate the arrays. Millimeter-sized plates that had assembled into disfavored orientations (such as the trans configuration for the [1,2,3,4] hexagons) dissociated freely under the levels of agitation we could generate without disrupting the interface, but the $100\ \mu\text{m}$ sized plates that had assembled into disfavored (but still energetically favorable) orientations did not appear to dissociate at any rate of agitation. Thus, the shear forces were weak relative to the lateral capillary forces for the $100\ \mu\text{m}$ hexagons, and the arrays that formed initially were stable to the agitation.

More ordered arrays could be assembled from the mm-sized hexagons than from the $100\ \mu\text{m}$ hexagons. To generate more ordered arrays of $100\ \mu\text{m}$ hexagons, either the strength of the lateral capillary forces should be lowered (by lowering the interfacial free energy of the liquid/liquid interface, by lowering the heights of the objects, or by lowering the size of the hydrophobic patch) or the strength of the forces opposing assembly should be

raised (by increasing the density of the objects or by using other methods of agitation).

To Generate Menisci Large Enough To Cause Assembly, the Objects Need Both Hydrophobic and Hydrophilic Faces. Objects with all the faces hydrophobic or hydrophilic will not perturb the interface sufficiently to generate menisci large enough to assemble. In this work we describe a method for generating the menisci by patterning the faces into hydrophobic and hydrophilic sets. Objects with both hydrophobic and hydrophilic faces will be pulled partly into the interface by the competing vertical capillary forces. They will, as a result, have menisci large enough to cause the objects to self-assemble into ordered arrays.

Future Directions. There are two general directions to proceed with in this work. (i) The sizes of the objects need to be decreased further. We believe that the methods outlined in this paper can be used to assemble objects with dimensions of $1-10\ \mu\text{m}$.⁹ In related work, we have generated 3D arrays of $10\ \mu\text{m}$ sized objects by capillary forces.⁴⁰ (ii) Larger, ordered crystals need to be assembled. Currently, we can assemble objects into arrays with short-range order but little long-range order. For many applications the size of the ordered crystal needs to be much larger than those we have obtained.

We believe that it will be possible to use capillarity as the basis for self-assembly in a range of functional structures such as MEMS, photonic band gap materials, crystal memories, and 3D microelectronics. This method of self-assembly has been used as a system to model biological systems such as receptor/ligand interactions and DNA/DNA duplex formation.^{6-8,14} The breadth of potential applications of the method will clearly be much greater if this method can be applied to μm -sized objects as well as to mm-sized objects.

Acknowledgment. This work was supported by the National Science Foundation (Grants CHE-9901358 and DMR-9809363) and the Defense Advanced Research Projects Agency. N.B. thanks the Department of Defense for a predoctoral fellowship. This work used MRSEC shared facilities supported by the NSF (Grant DMR-9809363).

LA0014470

(40) Clark, T.; Tien, J.; Whitesides, G. M., submitted.